Chemistry and Properties of Cycloheptatetraene in the Inner Phase of a Hemicarcerand

Ralf Warmuth* and Melissa A. Marvel[a]

Abstract: Low-temperature photolysis of phenyldiazirine, incarcerated inside a hemicarcerand which is built from two cavitands connected by four butane-1,4-dioxy linker groups, yields transient phenylcarbene; this carbene then undergoes ring photochemical expansion to cycloheptatetraene in low yield. Competitively, the transiently formed phenylcarbene reacts with the surrounding hemicarcerand. The yield of the photochemical ring expansion was increased when the photolysis was carried out inside a partially deuterated hemicarcerand. Two insertion products resulting from an intramolecular phenylcarbene insertion into an acetal C–H(D) bond or an α-C–H bond of a butane-1,4-dioxy linker group have been isolated and characterized. The measured isotope effect for insertion into an acetal C–H(D) bond at 15.5 K is consistent with a reaction of singlet phenylcarbene. Incarcerated cycloheptatetraene is stable for a limited time at 100 °C and almost infinitely stable at room temperature in the absence of oxygen. NOESY experiments provide the distance ratio $r_{21}/r_{23} = 1.134 \pm 0.01$ between protons H1 – H2 and H2 – H3 of cycloheptatetraene which is consistent with its twisted structure. Low-temperature photolysis of phenyldiazirine, incarcerated inside a chiral hemicarcerand which is built from two cavitands connected with three butane-1,4-dioxy and one (*S*,*S*)-2,3-*O*-isopropylidene-2,3-dihydroxybutane-1,4-dioxy linker group yields two diastereomeric cycloheptatetraene hemicarceplexes in a 2:3 ratio (30% total yield). Variable temperature ^{1}H NMR studies provided a lower limit of $\Delta G^{\ddagger} = 19.6$ kcal mol^{-1} for the enantiomerization barrier of cycloheptatetraene. Incarcerated cycloheptatetraene reacts rapidly with oxygen to yield benzene and carbon dioxide via the 1,2-dioxaspiro[2,6]nona-4,6,8-triene intermediate. Different mechanisms for the formation of this spirodioxirane intermediate are discussed based on the measured rate of the oxygen addition. The activation parameters for the decarboxylation of the spirodioxirane have been measured in different bulk solvents. The free energy of activation shows very little solvent dependency. However, a strong propensity for enthalpy – entropy compensation due to a solvent reorganization that accompanies the reaction coordinate is observed.

Keywords: carbenes · dioxiranes · hemicarcerands · molecular container compounds · strained molecules

Introduction

The gas-phase isomerization of phenylcarbene is a very important and fascinating carbene rearrangement.[1] At high temperature, phenylcarbene (**1**) undergoes ring expansion to cycloheptatetraene (**2**) (Scheme 1). The elucidation of the mechanism of the rearrangement of **1** and related arylcarbenes as well as the spectroscopic characterization of all postulated intermediates **1** – **4** has been a great challenge since its discovery more than 30 years ago.[2]

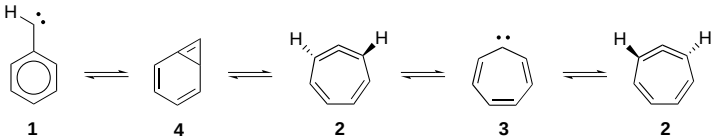

Scheme 1. Ring expansion observed for phenylcarbene (**1**) to cycloheptatetraene (**2**).

The identity of triplet phenylcarbene (^{3}**1**) and **2** have been firmly established spectroscopically in low-temperature matrices.[3] Chapman and co-workers photochemically generated ^{3}**1** in an argon matrix at 10 K.[3b,c] Upon further irradiation, ^{3}**1** rearranged to cycloheptatetraene which was characterized by UV/Vis and FT-IR spectroscopy. Matrix isolation of the pyrolysis products of phenyldiazomethane (**5**) confirmed that cycloheptatetraene is the ground state on this region of the

[a] Dr. R. Warmuth, M. A. Marvel
Department of Chemistry
Kansas State University, 111 Willard Hall
Manhattan, Kansas 66506-3701 (USA)
Fax: (+1) 785-532-6666
E-mail: warmuth@ksu.edu

Supporting information for this article is available on the WWW under http://www.wiley-vch.de/home/chemistry/ or from the author. ^{1}H NMR spectra of **9**·**12**, **10**·**12**, **15**·**12**, **16**·**12**, **15**·benzene, **21**, **22**, and **23**. DQF-COSY spectra of **20**, **23** and of a solution containing **10**·**25**. MALDI-TOF spectra of a solution containing **10**·**25**.

  0947-6539/01/0706-1209 $ 17.50+.50/0

C_7H_6 potential energy surface.[3c] Rapid dimerization upon warming the matrix prevented any mechanistic conclusions regarding the equilibrium between cycloheptatetraene and cycloheptatrienylidene **3**, which plays an essential role in the solution-phase chemistry of both intermediates **2** and **3**.[4] The missing spectroscopic evidence for bicycloheptatriene **4**,[3c] which is predicted as an intermediate in the phenylcarbene rearrangement by high level ab initio calculations,[5] posed questions on its importance in this rearrangement. Conclusive spectroscopic evidence for the participation of bicycloheptatrienes in arylcarbene rearrangements has only been provided for **6** and **7** in the related naphthylcarbene rearrangements (Scheme 2).[6]

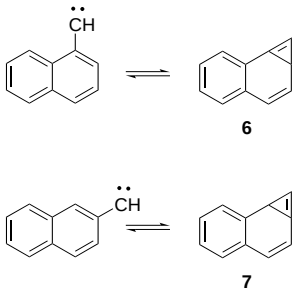

Scheme 2. Naphthylcarbene rearrangements.

Of particular interest are the energetics of the individual steps in the phenylcarbene rearrangement which strongly differ from those of the related phenylnitrene (**8**) rearrangement (Scheme 3).[1e, 7]

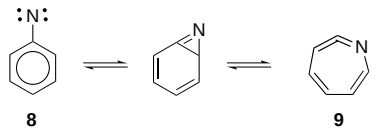

Scheme 3. Phenylnitrene (**8**) rearrangement.

Though ab initio calculations predict a high exothermicity of 16–18 kcal mol^{-1} for the ring expansion of **1** to **2**,[5] this rearrangement usually requires high temperatures unless **1** is produced with a tremendous amount of excess energy, for example, by the reaction of atomic carbon with benzaldehyde or benzene. Under these conditions it thermally expands even at 77 K as has been recently demonstrated by Shevlin and co-workers.[8] On the other hand, the related solution-phase rearrangement of phenylnitrene (**8**) to ketimine **9** takes place within one nanosecond at room temperature. Platz and co-workers measured the ring-expansion barrier of **8** to $E_a = 5.6 \pm 0.3$ kcal mol^{-1} and $A = 10^{13.1\pm0.3}$ s^{-1}.[9] This barrier is 7–9 kcal mol^{-1} lower than the calculated barrier for the ring expansion of **1** which is in the range of 13–15 kcal mol^{-1}.[5] One goal of our research efforts is the detailed spectroscopic investigation of the relevant intermediates in the phenylcarbene rearrangement and the experimental determination of all barriers on the phenylcarbene potential energy surface.

Recently, we reported on the first step towards our long-term goal.[10] We made use of the ability of molecular container compounds to shelter an incarcerated guest molecule from bulk-phase reactants, which allowed for the stabilization and spectroscopic characterization of cyclobutadiene and *o*-benzyne.[11–14] We observed photochemical ring expansion from **1** to **2** in the inner phase of hemicarcerand **9** and **10** (Scheme 4).[15]

Cycloheptatetraene (**2**) is stable even at temperatures up to 100 °C, while protected from dimerization by the surrounding host. During our investigation of the inner-phase chemistry of incarcerated **2**, we discovered an interesting new reaction of **2**. When we exposed **9**·**2** or **10**·**2** to oxygen, the incarcerated guest reacted rapidly to yield quantitatively benzene **11**. Here, we report on the inner-phase chemistry of phenylcarbene and cycloheptatetraene (**2**). In particular, we carried out a detailed mechanistic investigation of the reaction between **2** and oxygen.

Results and Discussion

Synthesis of phenyldiazirine hemicarceplexes: We prepared hemicarceplexes **9**·**12** and **10**·**12** in 83% and 80% yield by reacting the diol-hosts **13** and **14**, respectively, with butane-1,4-dimethylsulfonate and Cs_2CO_3 in HMPA in the presence of excess **12**.[16, 17] Using the same procedure but replacing butane-1,4-dimethylsulfonate with (−)-1,4-di-*O*-tosyl-2,3-*O*-isopropylidene-L-threitol gave hemicarceplexes **15**·**12** and **16**·**12** in 19% and 23% yield, respectively. The deuterated diol-host **14** was prepared from **17** as outlined in Scheme 5 using modified procedures reported for the preparation of **13**.[16, 18] The reaction of resorcinarene **17** with excess CD_2Cl_2 in DMF in the presence of K_2CO_3 at 80–85 °C for eight days afforded **18** in 50%.[18a] Cavitand **18** was converted to **14** as reported earlier for synthesis of the parent **13** from **19**.[16, 18]

Inner-phase photolysis of phenyldiazirine: The mechanism of the photochemical phenylcarbene rearrangement has been investigated by Chapman and co-workers in argon at

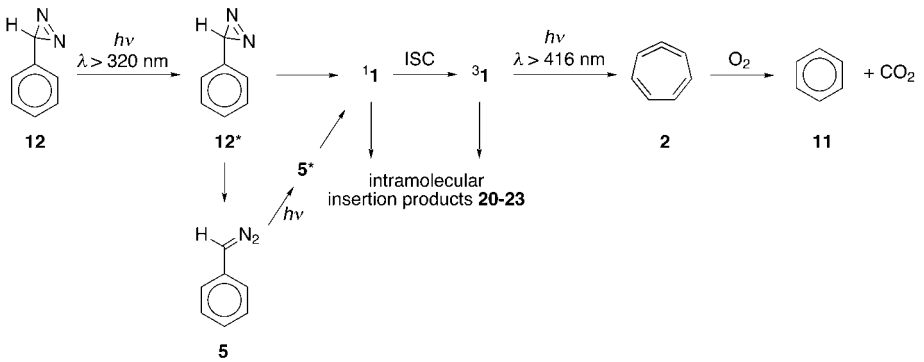

Scheme 4. Photochemical ring expansion from **1** to **2** in the inner phase of hemicarcerand **9** and **10**.

0947-6539/01/0706-1210 $ 17.50+.50/0 *Chem. Eur. J.* **2001**, *7*, No. 6

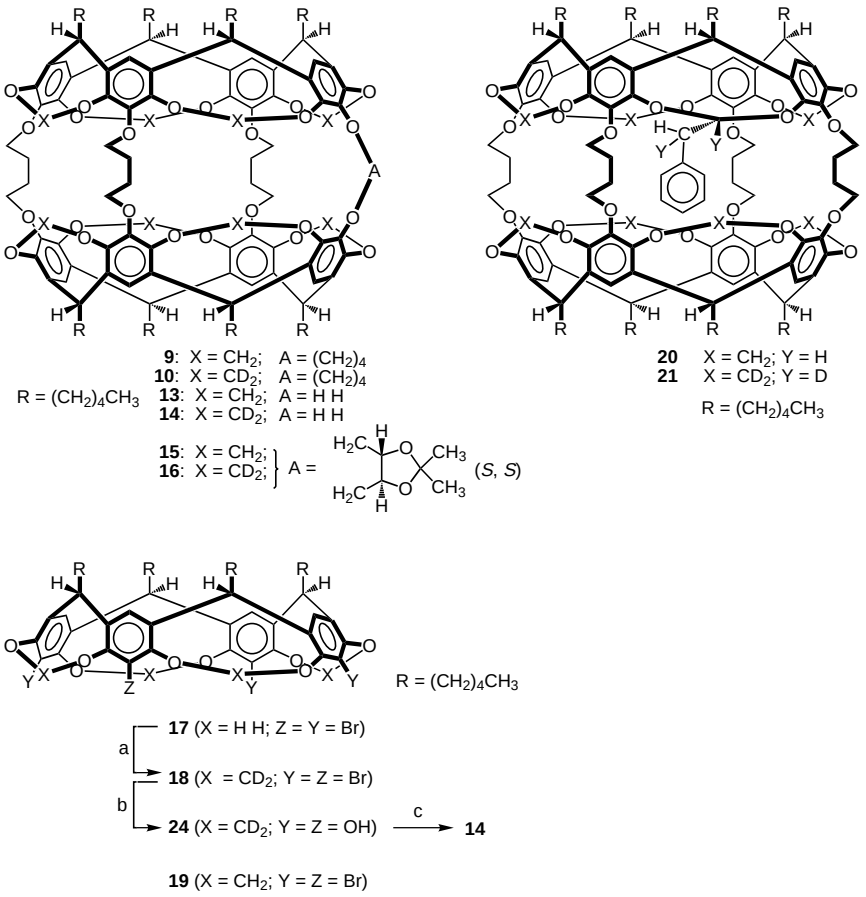

Scheme 5. Synthesis of various hemicarcerands: a) CD_2Cl_2, DMF, K_2CO_3, 80 °C, 8 d. b) 1) *n*BuLi, THF; 2) $B(OCH_3)_3$; 3) H_2O_2, OH^-. c) 3 equiv $MsO(CH_2)_4OMs$, NMP, Cs_2CO_3, 14 h, rt.

10 K.[3b–d] Photolysis of matrix-isolated **12** yields **5** and singlet phenylcarbene ^{1}**1** which rapidly undergoes intersystem crossing to triplet ^{3}**1**. Upon irradiation at 416 nm, ^{3}**1** undergoes ring expansion to **2**. The inner-phase photochemistry of **12** is similar. Brief irradiation (30 s, $\lambda > 320$ nm) of a solution of **9·12** in $CDCl_3$ at room temperature yielded a new hemicarceplex together with several other products, which result from intramolecular phenylcarbene insertions into **9**.[13b] After further photolysis (10 min) the new hemicarceplex was no longer detectable by ^{1}H NMR spectroscopy. We tentatively assign this hemicarceplex to the phenyldiazomethane hemicarceplex **9·5** based on its photosensitivity and the strong IR absorption at 2061.5 cm^{-1} (2055 cm^{-1}, in argon at 15 K),[3c] which is absent prior to and after prolonged photolysis. Due to its thermal instability, no attempts were undertaken to isolate **9·5**. The main product (57% yield) under these photolysis conditions was the intramolecular phenylcarbene insertion product **20**. This hemicarcerand results from an insertion of transiently formed **1** into a highly activated inward pointing acetal C–H bond of **9**. The structural assignment of **20** is based on the results of deuteration studies (see below) and on symmetry considerations. Insertion product **20** has C_s symmetry. Consistently, the ^{1}H NMR spectrum of **20** shows a set of four chemically different aryl protons H_a (ratio 2:2:2:2), six chemically different outward pointing acetal protons H_o (ratio 1:1:1:1:2:2), six chemically different methine protons H_m (ratio 1:1:1:1:2:2), and five chemically different inward pointing acetal protons H_i (ratio 1:1:1:2:2) (Figure 1). The protons of the inner-phase located benzyl group are assigned to multiplets at $\delta = 5.55$ (d), 4.90 (t), 3.65 (t, partially covered by an inward pointing acetal proton) and 1.20 (d) (ratio 2:2:1:2).

When we photolyzed a solution of **9·12** in toluene at 77 K, **20** was again the major product (84%). In some runs, small amounts (<2%) of the cycloheptatetraene complex **9·2** formed as well. Lowering the photolysis temperature to 15.5 K increased the yield of **9·2** (12.5%) and decreased that of **20** (83%). Higher yields of **10·2** and a greatly decreased amount of acetal C–D insertion resulted from the photolysis of the partially deuterated hemicarceplex **10·12** as a consequence of a kinetic isotope effect for this insertion (see Table 1). In the low temperature photolysis ($T = 77$ K) a second insertion products **22** and **23** formed in small amounts (Table 2 and Figure 2).

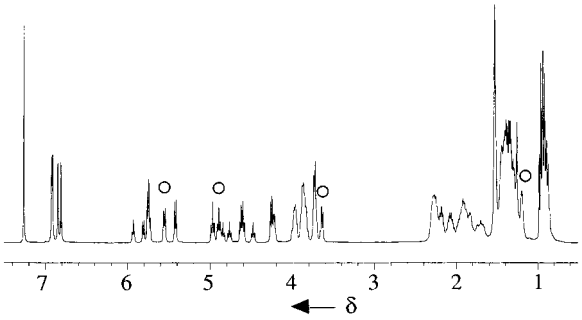

Figure 1. ^{1}H NMR spectrum (400 MHz, $CDCl_3$, 25 °C) of **20**: (○) protons of the inner-phase located benzyl group.

Table 1. Relative product yields [%][a] for the inner-phase photolysis of **12** inside hemicarcerands **9** and **10**.

T	Hemicarceplex	**9·2**	**10·2**	**20**	**21**	**22**	**23**	k_H/k_D
295 K	**9·12**	n.d.[b]		57		n.d.		
295 K	**10·12**		n.d.[b]		24		n.d.[b]	4.2
195 K	**9·12**	n.d.[b]		58		n.d.		
195 K	**10·12**		n.d.[b]		57		n.d.[b]	1
77 K	**9·12**	2		84		4.5		
77 K	**10·12**		18		60		13	3.5
15.5 K	**9·12**	12.5		83		2.5		
15.5 K	**10·12**		31		46		10	5.7

[a] Yields were determined by integration of selected signal of each compound in the room temperature ^{1}H NMR spectra of the photolyzed solutions and are based on the amount of formed phenylcarbene. [b] n.d.: not detected. NMR detection limit was approximately 1%.

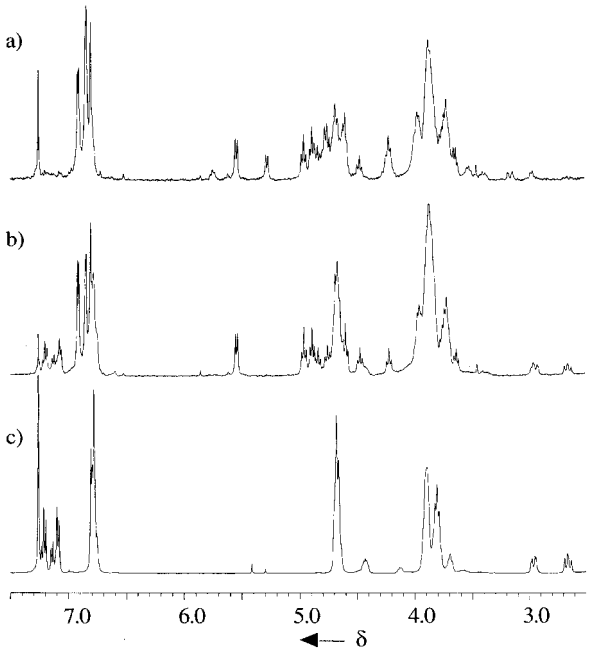

Figure 2. Partial ^{1}H NMR spectra (400 MHz, $CDCl_3$, 25 °C) of a) a solution of **10·12** immediately after irradiated extensively at 15.5 K with low intensity light ($\lambda > 320$ nm); b) the same solution recorded one day later, and c) **23**. The changes in spectra a) and b) are due to the inside–outside rotation of the intramolecularly fixed benzyl group of **23**.

These products arise from an insertion of **1** into an alpha-C–H bond of one of the hemicarcerand dioxybutane linker groups. After the insertion, the benzyl unit of **22** and **23** undergoes an *inside–outside rotation*, in which it rotates from the inner phase through an opening in the hemicarcerand shell into the bulk phase. This conformational isomerization is most likely driven by a release of torsional strain at the carbon at which the insertion took place. This inside–outside rotation could be followed by ^{1}H NMR spectroscopy and is accompanied by large chemical shift changes of the benzyl group protons.

We were very surprised to observe this product, since the alpha-C–H bonds of the 1,4-dioxybutane linkers are pointing away from the inner phase in all available X-ray crystal structures of **9**·guest.[15] This suggests that either the linker groups are conformationally mobile under cryogenic conditions, or that during the cooling to low temperature different linker conformations are frozen such that their alpha-C–H bonds are partially exposed to the inner phase.

The measured hemicarcerand induced upfield-shift of the guest protons in **9·12** suggests that the axis, which connects the *para*- and the diazirine-C of **12**, is aligned with the D_4 axis of **9** (Scheme 6).

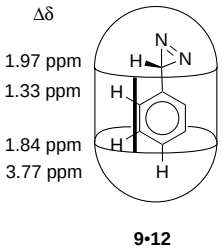

Scheme 6. Measured hemicarcerand induced upfield-shifts of the guest protons in **9·12**.

It is reasonable to assume that **1** will be generated in a similar orientation in which the carbene carbon is closer to the acetal hydrogens pointing inward as compared to the protons of the butanedioxy linker groups. Thus, **1** must be conformationally mobile at low temperatures to be able to form **22** and **23** as a consequence of the limited contractability of **9** and **10**. The inner phase of hemicarcerand **9** and **10** can be regarded as a "soft" hydrocarbon matrix which allows reactive intermediates to display some chemical selectivity and to distinguish C–H and C–D bonds in their intramolecular reactions.

From the measured product distributions listed in Table 1, we estimated the kinetic isotope effect k_H/k_D for the acetal C–H insertion of **1**. We assumed that under our photolysis conditions, all triplet ^{3}**1** is photochemically rearranged to **2**. Under this assumption, **20** and **21** are derived from singlet phenylcarbene. The ratio k_H/k_D can be calculated from the yields of **20** and **21** in the following Equation 1.

$$\frac{k_H}{k_D} = \frac{[\mathbf{20}] \times (1 - [\mathbf{21}])}{[\mathbf{21}] \times (1 - [\mathbf{20}])} \quad (1)$$

These calculated kinetic isotope effects at room temperature and below 77 K are slightly larger than the isotope effects for the reaction of phenylcarbene with cyclohexane and cyclohexene which have been measured earlier by Platz and co-workers.[19] The latter isotope effects are approximately 2 and 3 at room temperature and 77 K, respectively. From a product analysis which revealed the absence of typical triplet phenylcarbene derived products, Platz and co-workers concluded that they measured pure isotope effects for the reaction of singlet phenylcarbene. The difference between their isotope effects and the inner-phase isotope effects might be a consequence of the different nature of the C–H bonds involved. Alternatively, **20** and **21** might be partially triplet phenylcarbene derived which will result in a larger k_H/k_D ratio due to the expected larger isotope effect of ^{3}**1**.[20] This is a likely possibility since we know for sure that triplet phenylcarbene is formed in substantial amounts at 77 K or below.

Characterization of incarcerated cycloheptatetraene: In our previous communication, we reported a detailed spectroscopic characterization of incarcerated cycloheptatetraene.[10] In the ^{1}H NMR spectrum of a photolyzed solution of **10·2** recorded in [D_8]toluene at room temperature, we assign three multiplets at $\delta = 3.26$, 3.76 and 4.93 to the three chemically different protons of **2** (Table 2).

Table 2. Experimental (δ_{exptl}) and computed (δ_{calcd}) ^{1}H NMR chemical shifts of **2** and calculated host induced upfield shifts ($\Delta\delta$). Calculations were performed on the B3LYP/6-311G** optimized geometry of **2**.[23–25]

	δ_{exptl}	δ_{calcd} B3LYP/6-311G++(2d,2p)	$\Delta\delta$ HF/6-311G+(2d,p)	δ_{calcd}	$\Delta\delta$
H1/H1′	3.76	5.93	2.17	5.92	2.16
H2/H2′	3.26	6.38	3.12	6.32	3.06
H3/H3′	4.93	6.88	1.95	6.74	1.81

We were able to confirm our assignment by homonuclear COSY and NOESY spectra, which show cross signals between proton H1 and H2 and cross signals between protons H2 and H3 (Figure 3). In order to measure the relative internuclear distances between H2 and H1 (r_{21}) and H2 and H3 (r_{23}), we

0947-6539/01/0706-1212 $ 17.50+.50/0 *Chem. Eur. J.* **2001**, *7*, No. 6

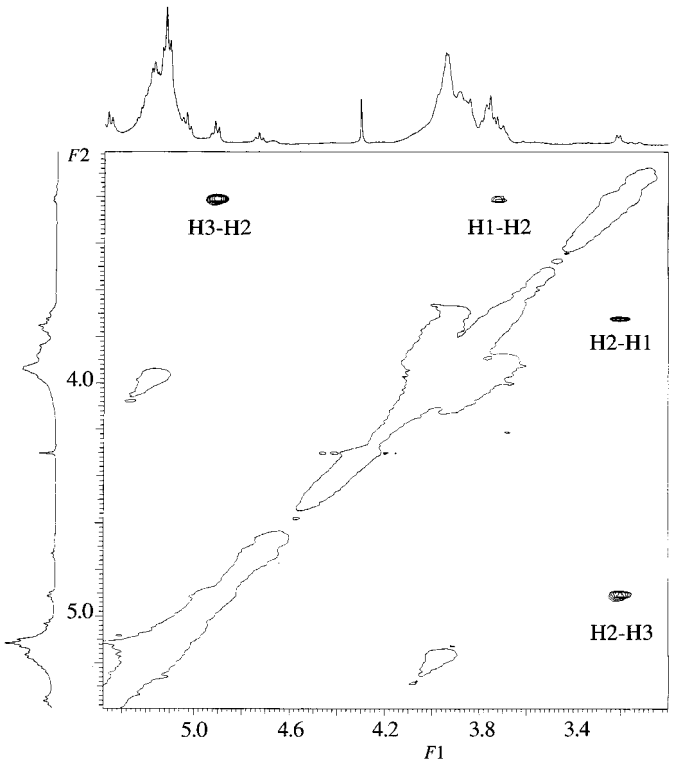

Figure 3. Partial NOESY spectrum (500 MHz, [D$_8$]toluene, 5 °C; t_{mix} = 1250 μs) of **10**·**12** after it has been irradiated ($\lambda > 320$ nm, 15.5 K). Cross peaks of the protons of incarcerated **2** are indicated.

recorded NOESY spectra with increasing mixing times (500–1250). In the region of initial linear built up of the cross peak intensities I_{21} and I_{23} in this three spin system, the internuclear distances can be calculated from the r_{xy}^{-6} dependence of I_{xy} according to Equation (2).[21]

$$\frac{r_{21}}{r_{23}} = \left[\frac{I_{21}}{I_{23}}\right]^{1/6} \qquad (2)$$

From the average cross peak intensity ratio at three different mixing times (750 ms, 1000 ms, 1250 ms) we determined a distance ratio $r_{21}/r_{23} = 1.134 \pm 0.01$. In Table 3 we have summarized the corresponding distance ratios extracted from

Table 3. Comparison between the calculated and the experimental distance ratio r_{21}/r_{23} in cycloheptatetraene (**2**).

Method	r_{21}/r_{23}	Δ	Ref.
exptl	1.134 ± 0.01		
BLYP/6-31G*	1.112	0.022	[5a]
B3LYP/6-31G*	1.120	0.014	[5c]
B3LYP/6-311G**	1.122	0.012	this work
CASSCF(8,8)/6-31G*	1.112	0.022	[5c]
MP2/6-31G*	1.124	0.01	[5b]

recent ab initio geometry optimizations of **1** at different levels of theory.[5, 22] The excellent agreement between the experimental and the predicted distance ratio is firm support for the successful inner-phase generation of **2**.

In addition, we have carried out GIAO calculations of the ^{1}H NMR chemical shifts of **2** based on its B3LYP/6-311G** geometry using the DFT and HF approach.[23–25] The calculated and experimental ^{1}H NMR chemical shifts together with the hemicarcerand induced shielding (Δδ) are listed in Table 2. The calculated Δδ values suggest an inner-phase orientation of **2** in which the strained allene bonds are facing an equatorially located opening in the hemicarcerand shell. This predicted orientation is important for the observed inner-phase chemistry of incarcerated **2**.

Inner-phase reactivity and barrier of enantiomerization of cycloheptatetraene: Despite the large strain energy, incarcerated **2** does not react with methanol or water in the bulk phase even at higher temperature (60 °C).[10] We speculated earlier that the non-reactivity of **2** is due to an unfavorable inner-phase equilibrium between **2** and **3**. The latter is known to react rapidly with alcohols in solution to yield the tropylium cation.[4a] Cycloheptatetraene enantiomerizes by the planar singlet **3**. Recent ab initio calculations have identified the open shell singlet $^1A_2$-**3** as a possible enantiomerization transition state structure.[5a,b] In order to measure the equilibrium constant between **2** and **3**, we generated **2** in the chiral inner phase of hemicarcerand **16**.[26] We anticipate that the resulting two diastereomeric hemicarceplexes **16**·(+)-**2** and **16**·(−)-**2** would be differentiable by ^{1}H NMR spectroscopy, thus allowing us to follow their thermal interchange through the guest enantiomerization.

Irradiation of a solution of **16**·**12** in [D$_8$]toluene (15.5 K, $\lambda > 320$ nm) gave **16**·(+)-**2** and **16**·(−)-**2** (total yield 30%) together with phenylcarbene insertion products. Fortunately, both diastereomeric hemicarceplexes formed in approximately equal amounts (ratio 2:3) and their guest protons H2, H2′ showed a small but discernible Δδ value of 15 Hz (Figure 4).

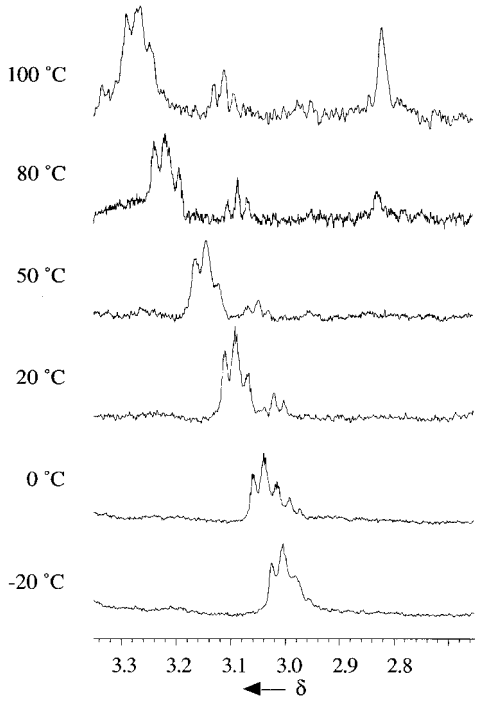

Figure 4. Partial ^{1}H NMR spectra (400 MHz, [D$_8$]toluene) at different temperatures showing the two partially overlapping multiplets, which are assigned to the cycloheptatetraene protons H2,H2′ of **16**·(+)-**2** and **16**·(−)-**2**.

Whether the diastereomeric excess of 20% results from asymmetric induction in the phenylcarbene ring expansion or from an inner-phase equilibration of the diastereomeric complexes is not clear and requires further investigations. Unfortunately, we could not induce coalescence of both signals even at 100 °C (Figure 4). From the absence of line broadening we conclude that the barrier must be higher than 19.6 kcal mol^{-1},[27] which sets a lower limit in agreement with all current calculations (Scheme 7).[5]

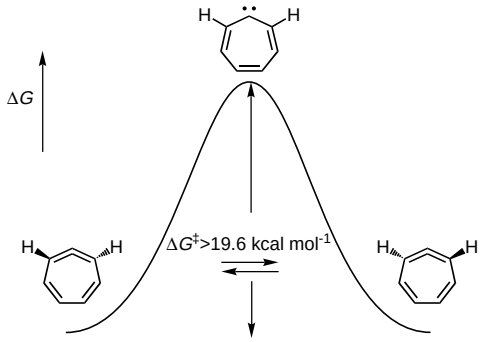

Scheme 7. Enantiomerization barrier.

Thus, the enantiomerization barrier must dependent strongly on the medium and must be lowered in polar environments such as alcohols which would favor the more polar **3** with a larger calculated dipole moment ($\mu = 1.26$ D, B3LYP/6-311++G**) as compared to **2** ($\mu = 5.07$ D, B3LYP/6-311++G**).[4c] In addition, it is likely that hydrogen-bond formation with an alcohol strongly stabilizes **3** as suggested by Borden and Karney.[28] Indeed, gas-phase DFT calculations (B3LYP/6-311++G** level of theory) predict a 8.5 kcal mol^{-1} stabilization of $^1A_1$-**3** upon hydrogen bonding to methanol,[23–25] whereas **2** and CH_3OH are only weakly bound ($\Delta E_{stab} = 0.6$ kcal mol^{-1} through an O-H/π interaction (Figure 5). This reduces the enantiomerization barrier by

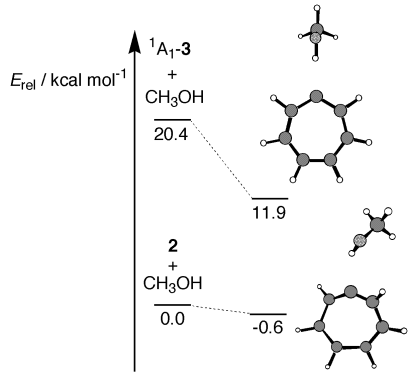

Figure 5. Stabilization of cycloheptatrienylidene and cycloheptatetraene upon hydrogen-bond formation with methanol. Relative energies (B3LYP/6-311++G**+ZPVE) are calculated at the B3LYP/6-311G** optimized geometries (**2**, $^1A_1$-**3** and CH_3OH) and at the B3LYP/6-31G* optimized geometries (**2**···$HOCH_3$ and $^1A_1$-**3**···$HOCH_3$ complex).

7.9 kcal mol^{-1}. Though the predicted inner-phase orientation of **2** exposes the allenic carbon to the bulk phase, steric interactions between the bulk-phase hydrogen-bond donor methanol and the atoms that line up the equatorial located portal of **10** might destabilize such a through-shell hydrogen-bonding interaction.

Inner-phase reaction of cycloheptatetraene with oxygen: When we exposed solutions containing **9·2** or **10·2** to the atmosphere, we observed a rapid reaction of **9·2** and **10·2** with oxygen which yields the benzene hemicarceplex and CO_2. The latter most likely escapes the inner phase and was detected by FT-IR spectroscopy. The formed benzene hemicarceplex was identified by its characteristic signal in the ^{1}H NMR spectrum of the reaction mixture and by comparison with an authentic sample prepared as published by Cram and co-workers.[14]

In order to elucidate the mechanism of this interesting reaction, we carried out low temperature ^{1}H NMR studies in the hope of detecting possible intermediates. Indeed, these studies revealed the formation of an intermediate hemicarceplex. When we purged a [D_8]toluene solution of **10·2** with air at −15 °C for two minutes and followed the fate of **10·2** at −10 °C by ^{1}H NMR spectroscopy, the proton signals assigned to **2** slowly disappeared and a new set of three multiplets appeared at $\delta = 6.43$ (m), 4.44 (d, $J = 11.8$ Hz), and 2.99 (m). The integral of each multiplet corresponds to two protons (Figure 6).

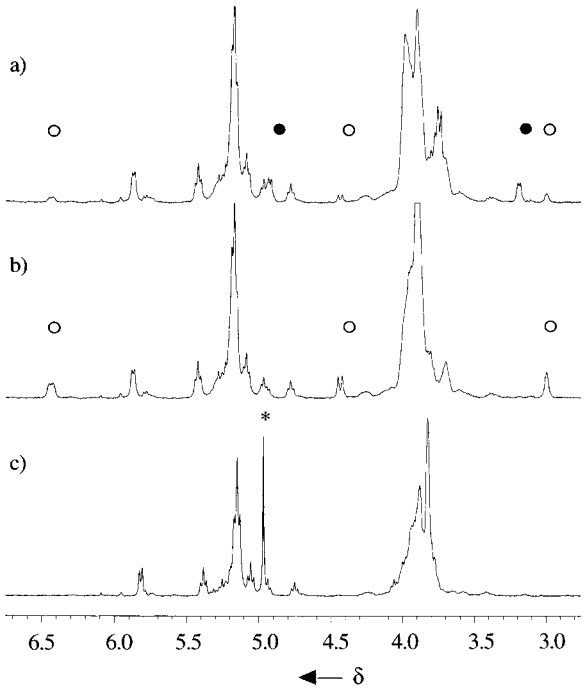

Figure 6. Partial ^{1}H NMR spectra (400 MHz) of a photolyzed solution of **10·12** in [D_8]toluene at −10 °C a) and b), and at 27.6 °C c): 3 min after the solution was saturated with air a), one hour later b), and after 90 min at 27.6 °C c); Peaks for the ^{1}H nuclei of incarcerated **2** (●), **25** (○), and benzene (*).

A DQF-COSY experiment showed cross peaks between the doublet at $\delta = 4.44$ and the multiplet at 6.43 and between the doublet at 4.44 and the multiplet at 2.99. Upon warming of

0947-6539/01/0706-1214 $ 17.50+.50/0 Chem. Eur. J. 2001, 7, No. 6

this solution to room temperature, the intermediate hemicarceplex decomposed quantitatively to **10**·benzene, which was identified by the characteristic singlet at 4.97 of the six benzene protons (Figure 6). The HR-MALDI-TOF mass spectrum of the above solution shows a isotopic cluster with the base peak at *m*/*z* 2138.192 which we assign to the ion [**10**·(**2**+O_2)+Na]$^+$. This ion is absent in the HR-MALDI-TOF MS recorded after the solution has been standing at room temperature for 2 h. At the same time, the intensity of the isotopic cluster of [**10**·benzene+Na]$^+$ increases by the same amount. The NMR spectroscopic and mass spectrometric data are only consistent with the guest of the intermediate hemicarceplex being either dioxirane **25** or tropone oxide **26** assuming fast rotation around the C–O bond of **26** on the NMR time scale. The absence of a strong UV/VIS absorption band in the region between 350 nm and 650 nm, which would be characteristic for carbonyl oxides[29] and which is predicted at λ_{max} 546 nm for **26**, excludes the latter as the guest structure.[30] Thus, all spectroscopic data are consistent with **25**. We assign the three multiplets at $\delta = 6.43$, 4.44, and 2.99 to the protons H2/H2′, H1/H1′, and H3/H3′ of **25**, respectively.

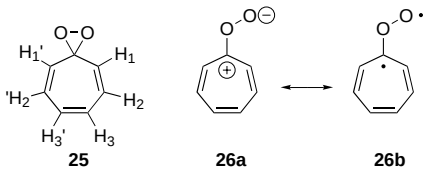

The formation of **25** involves the reaction of a singlet ground state reactant **2** with a triplet ground state reactant (O_2) which is an interesting situation. Similar spontaneous autoxidations in the absence of an initiator have been observed by Cram and co-workers for cyclobutadiene (**27**) incarcerated inside a hemicarcerand,[12] and by Maier and co-workers for the kinetically stabilized tri- (**28**),[31] and tetra-*tert*-butylcyclobutadiene (**29**).[32]

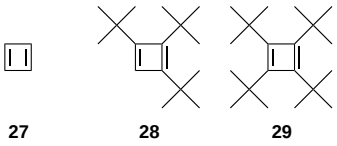

Even though a spin inversion is necessary somewhere along the reaction coordinate, both cyclobutadiene and **2** show extremely high reactivity towards oxygen. The fact that **2** can thermally rearrange to various intermediates on the C_7H_6 potential energy surface such as **1**, **3**, or **4**,[33] of which each could be the reacting species, makes the present case especially interesting. We have considered four different reaction pathways A–D for this autoxidation leading to **25** (Scheme 8). In pathway A, charge-transfer complex formation between triplet oxygen $^3O_2$ and **2** induces an intersystem crossing (ISC) of the former to yield singlet oxygen $^1O_2$. Dioxirane **25** is formed either via an allowed side-on [2+8] addition between $^1O_2$ and **2** or alternatively via an end-on [2+8] addition followed by the thermal cyclization of the

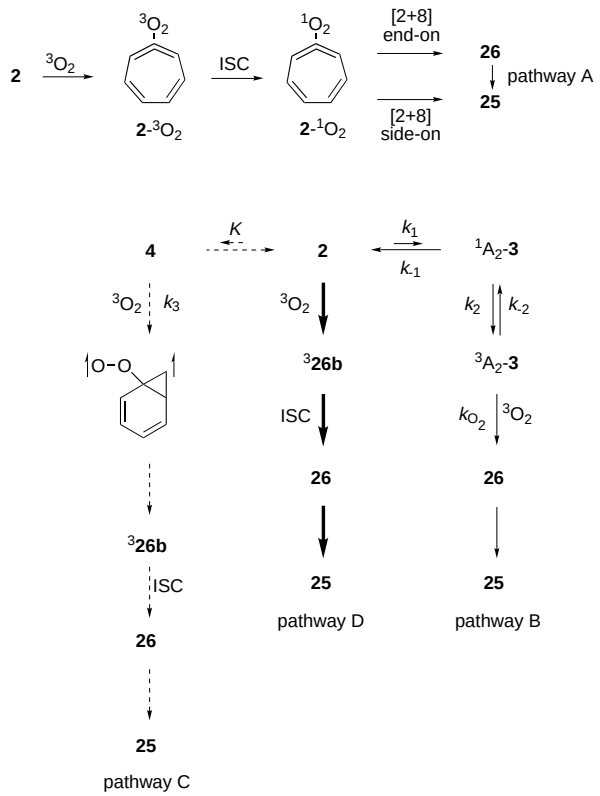

Scheme 8. Reaction pathways A–D for the autoxidation leading to **25**.

resulting tropone oxide **26** (Scheme 8, pathway A). Such a thermal intersystem crossing of $^3O_2$ induced by charge-transfer complex formation between $^3O_2$ and the highly strained 3,3,6,6-tetramethyl-1-thia-4-cycloheptyne (**30**) was observed earlier by Krebs and co-workers (Scheme 9).[34, 35]

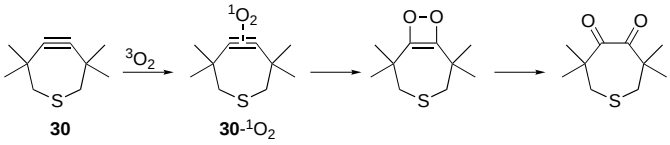

Scheme 9. Thermal intersystem crossing of $^3O_2$ induced by charge-transfer complex formation between $^3O_2$ and the highly strained 3,3,6,6-tetramethyl-1-thia-4-cycloheptyne (**30**).[34, 35]

Consistent with this mechanism is the lower limit of the activation barrier $E_a = 21$ kcal mol^{-1} measured[35] which is similar to the singlet–triplet splitting of molecular oxygen $E_{ST} = 22.54$ kcal mol^{-1},[36] and the successful trapping of transiently formed singlet oxygen with tetramethylethylene.

In the present reaction, attempts to trap transiently produced singlet oxygen with furan in the bulk solvent failed. A comparison of the relative reaction rates shows further major differences between the reaction of **2** and of **30** with oxygen. The rate of the reaction between oxygen and **10**·**2** is first order in the concentration of oxygen. The measured bimolecular rate constant k_{O_2+2} in $CDCl_3$ at 263 K is $k_{O_2+2} = 5.6 \times 10^{-4}$ mol^{-1} s^{-1}. At the same temperature, the rate constant of the addition of oxygen to **30** is about five orders of magnitude slower (k_{O_2+30} (263 K) $\approx 1 \times 10^{-8}$ mol^{-1} s^{-1}).[34] The

latter rate was estimated from the experimental activation energy and the room temperature rate constant in oxygen saturated CCl_4 ($k_{O_2+\mathbf{30}}$ (295 K) $\approx 1 \times 10^{-6}$ mol^{-1} s^{-1}).[34, 35] Both reactions should have similar activation barriers of about $E_a = 22$ kcal mol^{-1}. This would lead to a positive estimated activation entropy $\Delta S^{\neq} = 8$ e.u., which is unlikely for a reaction that requires the formation of an ordered charge-transfer complex. In pathway B, triplet $^3O_2$ reacts with triplet cycloheptatrienylidene, for example, $^3A_2$-**3**. Triplet $^3A_2$-**3** is predicted to lie approximately 2–5 kcal mol^{-1} above $^1A_2$-**3**, which is the possible enantiomerization transition state structure of **2**.[5a,b] Based on this small singlet–triplet gap and the similar geometries of $^1A_2$-**3** and $^3A_2$-**3**, intersystem crossing between both states would be extremely fast and would provide a very efficient route for the equilibration of **2** and $^3A_2$-**3**. The expected experimental rate constant k_{exptl} for this reaction pathway is given by Equation (3).[37]

$$k_{exptl} = K_{eq} k_{O_2} \quad (3)$$

$K_{eq} = k_1 k_2 / k_{-1} k_{-2}$ is the equilibrium constant between $^3A_2$-**3** and **2**. Assuming a rate constant $k_{O_2} = 10^{-9}$ mol^{-1} s^{-1} typical for the reaction of triplet carbenes with oxygen,[29] the measured rate constant $k_{exptl} = 5.6 \times 10^{-4}$ mol^{-1} s^{-1} at 263 K allows us to estimate K_{eq} and thus the free energy difference ΔG(263 K) between $^3A_2$-**3** and **2** is ΔG(263 K) = 14.8 kcal mol^{-1}.

Clearly, ΔG(263 K) is much lower than our measured lower limit of the enantiomerization barrier of **2** which is contradictory and excludes the participation of $^3A_2$-**3** or any other triplet state of **3** in this autoxidation. For a similar reason, reaction pathway C, in which the autoxidation is initiated by a reaction of $^3O_2$ with **4**, can be excluded. Bicycloheptatriene (**4**) is predicted as an intermediate in the thermal equilibration between cycloheptatetraene and phenylcarbene. Recent ab initio calculations place **4** approximately 15–17 kcal mol^{-1} above **2**. Assuming, that the reaction between $^3O_2$ and **4** is rate-controlling in pathway C, which leads to a reaction rate constant $k_{exptl} = K \cdot k_3$, requires a rate constant k_3 at the diffusion limit. We regard this as very unlikely. Therefore, triplet oxygen must add directly to the allenic carbon of **2** to give triplet biradical **26a**, which cyclizes after a singlet–triplet intersystem crossing (pathway D).[38] Though a thermal carbonyl oxide–dioxirane equilibrium has not been observed in condensed phases, the barrier for cyclization of **26** is expected to be substantially lower compared with formaldehyde oxide H_2COO (activation energy = 20.3–24.0 kcal mol^{-1})[39] due to the smaller double bond character of the C–O bond of **26**.[30]

The answer to the question why **2** is so reactive towards triplet oxygen and the nature of the initializing step of the autoxidation of **2** is not clear, yet. Maier and co-workers suggested an initial electron transfer step in the biradical type reactivity of cyclobutadiene.[31c] An electron transfer from a strained olefinic bond to $^3O_2$ to produce radical ions or a charge-transfer complex has also been postulated by Bartlett and Banavali in the spontaneous autoxidation of various strained cyclic olefins.[40] We are currently studying related systems, which will hopefully provide more insight into this interesting reaction.[41]

It is reasonable to assume that the thermal decarboxylation of **25** involves an initial electrocyclization of **25** to norcaradiene (**31**) followed by the homolytic cleavage of the O–O bond and the cheletropic extrusion of CO_2 as shown in Scheme 10.

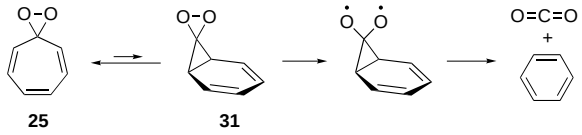

25 **31**

Scheme 10. Decarboxylation of **25**.

In order to support this mechanism, we determined the activation parameters, E_a and A, from the temperature dependence of the rates of decarboxylation (Figure 7 and Table 4). At all temperatures and in all bulk solvents, we observed first-order kinetics.

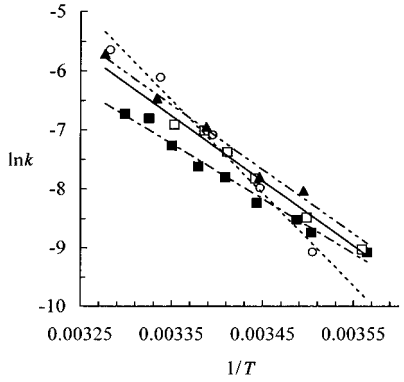

Figure 7. Arrhenius plots of the decarboxylation of **10**·**25** in different bulk solvents: $CDCl_3$ (□; ——); [D$_8$]toluene (■, — -); [D$_8$]THF (○, - - - -); CH_2Cl_2 (▲; — - -).

Table 4. Activation parameters for the decarboxylation of **10**·**25** in different bulk solvents.

Solvent	E_a	log$A$	$\Delta G^{\neq}$ (298 K)	$\Delta H^{\neq}$ (298 K)	$\Delta S^{\neq}$ (298 K)	$T\Delta S^{\neq}$ (298 K)
[D$_8$]THF[a]	31.5	20.1	21.45	30.9	31.7	13.4
$CDCl_3$[a]	22.1	13.1	21.62	21.5	– 0.5	– 0.95
[D$_8$]toluene[a]	18.7	10.5	21.9	18.1	– 12.7	– 3.93
CH_2Cl_2[b]	21.9	13.0	21.52	21.3	– 0.8	– 1.3

[a] Measured by ^{1}H NMR spectroscopy. [b] Measured by normal-phase HPLC.

We noticed interesting aspects regarding these activation parameters:

1. The free activation energies $\Delta G^{\neq}$ in the different solvents are almost identical ($\Delta\Delta G^{\neq} \leq 0.45$ kcal mol^{-1}).
2. The enthalpy and entropy contributions to $\Delta G^{\neq}$ vary among the different solvents by as much as 13 kcal mol^{-1}.

We explain the solvent dependence of the activation parameters with a strong propensity of this inner-phase reaction towards enthalpy–entropy compensation due to a solvent reorganization.[42, 43] A solvent reorganization is expected if a

0947-6539/01/0706-1216 $ 17.50+.50/0 *Chem. Eur. J.* **2001**, *7*, No. 6

conformational change of the host (e.g., a twisting,[44] bending, elongation or contraction) accompanies the reaction coordinate. It is obvious that the transition state of the decarboxylation will have a very different shape and size as compared to **25**. Thus, host **10** will react to the change of the guest with a change of its own shape and size, in order to maximize the host–guest interactions. The increased (decreased) surface area of **10** will require more (less) solvent molecules for a complete solvation leading to a decrease (increase) of $\Delta H^{\neq}$ due to solvent–host interactions which is accompanied with an increase (decrease) of $T\Delta S^{\neq}$ by an equal amount due to the higher order of the solvent molecules in the solvation shell as compared to the bulk.[43] Interestingly, many enzymes display isokinetic behavior for their substrate binding steps and also for the catalyzed transformation inside their binding cavities.[45] As in the present case, this behavior has been explained with a conformational change of the enzyme that accompanies the substrate binding or reaction step. Thus molecular containers display enzyme type behavior in their inner-phase reactions. The fact that the different Arrhenius plots don't exactly cross at a common point suggests that this inner-phase decarboxylation possibly exhibits a small solvent effect as a result of a small dipole moment change of the hemicarceplex upon approaching the transition state. For example, the overall dipole moment of the hemicarceplex will change during a bending motion of the surrounding host, which has no net dipole moment if in a straight conformation, and/or from a dipole moment change of the reacting guest.

Since $\Delta G^{\neq}$(inner phase) is only slightly affected by the bulk medium, it is readily comparable with the free energy of activation in the gas or liquid phase $\Delta G^{\neq}$. This allows one to probe the influence of the host on an inner-phase reaction rate. Unfortunately, an experimental $\Delta G^{\neq}$ for the decarboxylation of free **25** is not available. We are currently exploring methods to generate **25** in the inner phase of a container compound and subsequently release the guest into the bulk in order to study its bulk phase decomposition kinetics.

Experimental Section

General: All reactions were conducted under argon unless noted otherwise. Tetrahydrofuran (THF) was freshly distilled from benzophenone ketone just prior to use. Hexamethylphosphoric triamide (HMPA) was dried over activated molecular sieves (4 Å). Dimethylformamide (DMF) and 1-methyl-2-pyrrolidinone (NMP) were purified by filtration through activated aluminum oxide and silica gel. ^{1}H NMR spectra were recorded on a 500 MHz or a 400 MHz Varian FT NMR spectrometer. ^{13}C NMR spectra were recorded on a 200 MHz Varian FT NMR spectrometer. Spectra were recorded in $CDCl_3$, [D_8]toluene or [D_8]THF and referenced to residual $CHCl_3$, [D_7]toluene or [D_7]THF at $\delta = 7.26$, 2.09, or 3.58, respectively. The temperature of the NMR spectrometer was calibrated with methanol (below 310 K) and ethylene glycol (above 310 K) temperature standards using calibration curves implemented in the Varian NMR software. FAB-MS were determined on a ZAB SE instrument with 3-nitrobenzyl alcohol (NOBA) matrix. MALDI-TOF mass spectra were obtained on an Ion Spec HiResMALDI mass spectrometer. FT-IR spectra were recorded on a Nickolet 580B with a Model 3600 station. CHN elementary analysis were obtained from Desert Analytics, Tuscon, Arizona. Gravity chromatography was performed on Bodman silica gel (70–230 mesh). Thin-layer chromatography involved aluminum-backed plates (silica gel 60 F_{254}, 0.25 mm).

Cavitand 18: Tetrabromoresorcinarene (**17**, 3 g, 2.77 mmol) was placed in a heavy wall pyrex tube containing a magnetic stirring bar and was dissolved in degassed dry DMF (25 mL) under argon. Anhydrous K_2CO_3 (5.5 g) and CD_2Cl_2 (5.5 mL, 99.6%, Cambridge Isotope Laboratories) were added. The tube was sealed and stirred at 80–85 °C for 8 d. After the reaction mixture was cooled to 0 °C, the tube was opened and the precipitated product was filtered off and washed with DMF (5 mL) and water (3 × 50 mL). The crude product was dried under vacuum, redissolved in the minimum amount of CH_2Cl_2 and purified by column chromatography (silica gel, CH_2Cl_2/hexane 1:1 *v*:*v*) to yield **18** (1.56 g, 50%). ^{1}H NMR (400 MHz, $CDCl_3$, 25 °C): $\delta = 7.03$ (s, 4H, aryl*H*), 4.85 (t, 4H, C*H*), 2.20 (dt, 8H, CHCH_2), 1.48–1.3 (m, 24H, $CH_2CH_2CH_2CH_2CH_3$), 0.92 (t, 12H, CH_3); ^{13}C NMR (50.29 MHz, $CDCl_3$, 22 °C): $\delta = 152.4$, 139.6, 119.4, 113.9, 98.1 (vb), 37.9, 32.1, 30.1, 27.7, 22.9, 14.3; HR-MS: calcd for $C_{52}H_{52}O_8D_8Br_4$: 1136.151; found: 1136.164 $[M]^+$.

Cavitand 24 was synthesized from **18** in 77% yield according to a procedure published by Cram and co-workers for the synthesis of the parent non-deuterated cavitand.[17b] ^{1}H NMR (400 MHz, $CDCl_3$, 25 °C): $\delta = 6.63$ (s, 4H, aryl*H*), 5.4 (brs, 4H, O*H*), 4.69 (t, 4H, C*H*), 2.17 (dt, 8H, CHCH_2), 1.48–1.3 (m, 24H, $CH_2CH_2CH_2CH_2CH_3$), 0.91 (t, 12H, CH_3); ^{13}C NMR (50.29 MHz; $CDCl_3$, 22 °C): $\delta = 142.3$, 141.1, 138.9, 110.5, 37.1, 32.3, 29.8, 27.8, 22.9, 14.3; HR-MS: calcd for $C_{52}H_{56}O_{12}D_8$: 911.478; found: 911.479 $[M]^+$.

Hemicarcerand 14 was prepared from **17** in 22% yield according to a procedure published by Cram and co-workers for **13**.[15] ^{1}H NMR (400 MHz, $CDCl_3$, 25 °C): $\delta = 6.79$ (s, 2H, aryl*H*), 6.76 (s, 4H, aryl*H*), 6.57 (s, 2H, aryl*H*), 4.68 (t, 4H, C*H* methine), 4.66 (t, 4H, C*H* methine), 3.96–3.78 (m, 12H, OCH_2CH$_2$), 2.23–2.08 (m, 16H, CHCH_2CH$_2$), 1.98 (brs, 8H, OCH$_2$CH_2), 1.94 (brs, 4H, OCH$_2$CH_2), 1.5–1.3 (m, 48H, CHCH$_2$CH_2CH$_2$CH_2CH$_2$CH$_3$), 0.89–0.95 (m, 24H, CH_3); ^{13}C NMR (50.29 MHz, $CDCl_3$, 22 °C): $\delta = 149.1$, 148.9, 148.8, 144.7, 144.3, 142.3, 141.2, 139.5, 139.2, 139.1, 138.6, 114.5, 110.4, 99.3 (vb), 74.1, 72.9, 37.2, 37.1, 32.3, 30.0, 29.9, 27.9, 27.8, 27.3, 26.9, 22.9, 14.3; HR-MS: calcd for $C_{116}H_{130}O_{24}D_{16}Na$: 1962.108; found: 1962.109 $[M+Na]^+$.

Hemicarceplex 9·12: A suspension of **13** (152 mg, 0.063 mmol), butane-1,4-dimethylsulfonate (147 mg, 0.6 mmol), anhydrous Cs_2CO_3 (750 mg) and phenyldiazirine (200 μL)[16] in dry HMPA (10 mL) was stirred under argon at room temperature in the dark for 3.5 d. The reaction mixture was pipetted into brine (50 mL) and filtered. The collected precipitate was washed with water (2 × 5 mL) and methanol (2 × 5 mL) and redissolved in $CHCl_3$ (10 mL). After the evaporation of the solvent, the residual crude product was dried under vacuum for 30 min, redissolved in the minimum amount of CH_2Cl_2 and purified by column chromatography (silica gel, CH_2Cl_2) to yield **9·12** as a white powder (133.5 mg, 80.6%). The hemicarceplex was stored at −25 °C, where it was stable without detectable decomposition for several months. ^{1}H NMR (400 MHz, $CDCl_3$, 25 °C): $\delta =$ 6.88 (s, 8H, aryl*H*), 5.61 (d, 8H, OCH_{outer}HO), 5.55 (d, 2H, *o*-aryl-*H* of guest), 5.05 (t, 2H, *m*-aryl-*H* of guest), 4.70 (t, 8H, C*H* methine, host), 4.12 (d, 8H, OCH_{inner}HO), 3.85 (brs, 16H, OCH_2CH$_2$), 3.13 (t, 1H, *p*-aryl-*H* of guest), 2.24–2.16 (m, 16H, CHCH_2CH$_2$), 1.86 (brs, 16H, OCH$_2$CH_2), 1.5–1.3 (m, 48H, CHCH$_2$CH_2CH$_2$CH_2CH$_2$CH$_3$), 0.93 (t, 24H, CH_3), 0.09 (s, 1H, C*H*-methine, guest); ^{13}C NMR (50.29 MHz, $CDCl_3$, 22 °C): $\delta = 148.9$(H), 144.5 (H), 139.4 (H), 135.8 (G), 127.7 (G), 126.2 (G), 123.2 (G), 114.7 (H), 98.6 (H), 72.3 (H), 37.2 (H), 32.3 (H), 30.2 (H), 27.9 (H), 27.7 (H), 22.9 (H), 21.5, 14.3 (H); FAB-MS (NBA-matrix): *m*/*z* (%): 2095.6 (30) $[M+H]^+$, 2067.7 (100) $[M-N_2-H]^+$; elemental analysis calcd (%) for $C_{127}H_{158}N_2O_{24}$: C 72.75, H 7.60, N 1.34; found: C 72.93, H 7.47, N 1.15.

Hemicarceplex 10·12 was prepared from **14** in 80% yield as described for the synthesis of **9·12** from **13**. ^{1}H NMR (400 MHz, $CDCl_3$, 25 °C): $\delta = 6.89$ (s, 8H, aryl*H*), 5.55 (d, 2H, *o*-aryl-*H* of guest), 5.05 (t, 2H, *m*-aryl-*H* of guest), 4.70 (t, 8H, C*H* methine, host), 3.85 (brs, 16H, OCH_2CH$_2$), 3.12 (t, 1H, *p*-aryl-*H* of guest), 2.24–2.16 (m, 16H, CHCH_2CH$_2$), 1.86 (brs, 16H, OCH$_2$CH_2), 1.5–1.3 (m, 48H, CHCH$_2$CH_2CH$_2$CH_2CH$_2$CH$_3$), 0.93 (t, 24H, CH_3), 0.10 (s, 1H, C*H*-methine, guest); FAB-MS (NBA-matrix): *m*/*z* (%): 2111.7 (50) $[M+H]^+$, 2083.7 (100) $[M-N_2+H]^+$, 1994.2 (60) $[M-$ **12**$+H]^+$.

Hemicarceplex 15·12 was prepared in 19% yield from **13** as described for **9·12** with the exception that (*S*,*S*)-(−)-1,4-di-*O*-tosyl-2,3-*O*-isopropylidene-L-threitol was used instead of butane-1,4-dimethylsulfonate. ^{1}H NMR (400 MHz, $CDCl_3$, 25 °C): $\delta = 6.9–6.8$ (m, 8H, aryl*H*), 5.72–5.5 (m, 8H, OCH_{outer}HO), 5.46 (d, 2H, *o*-aryl-*H* of guest), 4.95 (t, 2H, *m*-aryl-*H* of guest), 4.72 (t, 4H, C*H* methine, host), 4.68 (t, 4H, C*H* methine, host), 4.37 (d, 2H), 4.2–3.63 (m, 24H), 3.02 (t, 1H, *p*-aryl-*H* of guest), 2.3–1.7

(m, 28H), 1.5–1.3 (m, 48H, $CHCH_2CH_2CH_2CH_2CH_3$), 1.31 (s, 6H, CH_3), 1.0–0.85 (m, 24H, CH_3), 0.01 (s, 1H, C*H*-methine, guest); FAB-MS (NBA-matrix): *m*/*z* (%): 2167.7 (34) $[M+H]^+$, 2142.0 (100) $[M-N_2+H]^+$; elemental analysis calcd (%) for $C_{130}H_{162}N_2O_{26}$: C 71.99, H 7.53, N 1.29; found: C 71.78, H 7.37, N 1.28.

Hemicarceplex 16·12 was prepared in 23% yield from **14** as described for the synthesis of **15·12** from **13**. ^{1}H NMR (400 MHz, $CDCl_3$, 25 °C): δ = 6.9–6.8 (m, 8H, aryl*H*), 5.46 (d, 2H, *o*-aryl-*H* of guest), 4.95 (t, 2H, *m*-aryl-*H* of guest), 4.72 (t, 4H, C*H* methine, host), 4.68 (t, 4H, C*H* methine, host), 4.37 (d, 2H), 4.2–3.63 (m, 16H), 3.02 (t, 1H, *p*-aryl-*H* of guest), 2.3–1.7 (m, 28H), 1.5–1.3 (m, 48H, $CHCH_2CH_2CH_2CH_2CH_3$), 1.31 (s, 6H, CH_3), 1.0–0.85 (m, 24H, CH_3), 0.01 (s, 1H, C*H*-methine, guest); FAB-MS (NBA-matrix): *m*/*z* (%): 2185.1 (56) $[M+H]^+$, 2155.7 (100) $[M-N_2+H]^+$.

Hemicarceplex 15·benzene: A suspension of diol **13** (31 mg, 16 mmol), (*S*,*S*)-(−)-1,4-di-*O*-tosyl-2,3-*O*-isopropylidene-L-threitol (35 mg, 74 mmol) and Cs_2CO_3 (200 mg) in degassed anhydrous DMF (4 mL) was stirred for 2.5 d at 50–55 °C under argon. The reaction mixture was poured into water (30 mL). The precipitate was filtered off, washed with methanol (2 mL), dried at high vacuum overnight and then dissolved in benzene (2 mL). The benzene solution is sealed in a pyrex tube and is heated to 130 °C for 3 d. After the solution had cooled to room temperature, the tube was opened and the benzene solution was concentrated. The crude hemicarceplex was purified by column chromatography (silica gel, CH_2Cl_2) to yield **15·**benzene as a white powder (18 mg, 68%). ^{1}H NMR (400 MHz, [D_8]toluene, 15 °C): δ = 7.3–7.2 (m, 8H, aryl*H*), 5.84 (m, 2H, $OCH_{outer}HO$), 5.80 (m, 2H, $OCH_{outer}HO$), 5.76 (m, 2H, $OCH_{outer}HO$), 5.65 (m, 2H, $OCH_{outer}HO$), 5.2–5.05 (m, 8H, C*H* methine, host), 4.37 (d, 2H), 4.2–3.63 (m, 24H), 4.82 (s, 6H, guest-H), 4.40 (d, 2H), 4.33 (d, 2H), 4.31 (d, 2H), 4.25–4.1 (m, 16H), 3.68 (t, 2H), 3.5–3.4 (m, 4H), 3.38 (t, 2H), 2.44–2.14 (m, 28H), 1.65–1.2 (m, 54H, $CHCH_2CH_2CH_2CH_2CH_3$; linker CH_3), 1.0–0.8 (m, 24H, CH_3); ^{13}C NMR (50.29 MHz, $CDCl_3$, 22 °C): δ = 149.3, 149.2, 149.0, 148.8, 148.6, 148.2, 145.3, 145.1, 144.6, 139.5, 139.4, 139.3, 139.2, 139.1, 127.1 (*guest*), 114.8, 114.4, 114.2, 114.1, 110.3, 99.5, 99.4, 78.7, 74.6, 74.5, 74.2, 37.3, 32.4, 30.3, 30.1, 28.4, 28.0, 26.8, 23.0, 14.4; HR-MS: calcd for $C_{129}H_{162}O_{26}Na$: 2150.125; found: 2150.123 $[M+Na]^+$.

Photolysis experiments

General: In all photolysis experiments, samples were irradiated with the output of an Oriel Hg Power-Max lamp operating at 200 W (photolysis at T = 77 K) or at 115–120 W (photolysis at 15.5 K). A 10 cm water-filter and a 320 nm cut-off filter (WG320) was placed between the lamp and the sample.

Sample preparation: A solution of **9·12** or **10·12** (2–4 mg) in [D_8]toluene (150–200 μL for the photolysis at 15.5 K, otherwise 550 μL) was placed in a pyrex NMR tube and degassed by four freeze–pump–thaw cycles under vacuum. The NMR tube was sealed off under vacuum.

Photolysis at 77 K: Sample cooling was achieved with liquid nitrogen in a partially silvered dewar. The sample tube was placed in the light beam such that the bottom part of the frozen solution was in the focal point (4–5 mm diameter). First, the front of the sample was irradiated for 10 min, followed by further 10 min irradiation after the sample tube had been turned by 180°. During this irradiation the upper part of the frozen solution was protected from the light beam. After each 2 × 10 min irradiation period, the sample was moved downwards in 5 mm steps until all of the frozen solution had been irradiated (typically 6–7 vertical steps).

Photolysis experiments at lower temperatures: Cooling of the sample was achieved with a Cryogenics Closed Cycle Laboratory System Model CWS-202 (APD Cryogenics), which had been modified for this purpose. We designed a sample holder, which was made out of high purity copper and which allowed cooling of up to 250 μL of a solution sealed inside an NMR tube. The sample holder was screwed onto the top the expander. We placed an indium gasket between holder and expander for optimal thermal conductivity between both. In order to accommodate the sealed NMR tube, an eight inch long, stainless steel tube (8 mm inner diameter) was welded onto the upper port of the vacuum shroud. Irradiation of the sample was performed through a quartz window in the vacuum shroud. Prior to the photolysis, the lamp position was adjusted such that the sample was exactly in the focal point of the light beam. In a typical photolysis experiment, the solution was cooled in the dark to about 11–12 K. The irradiation of the frozen solution was performed as described for the photolysis at 77 K except that the irradiation time was reduced to each time 5 min and that the sample tube was moved every 5 min 2.5 mm downwards in the light beam (total 5–6 times 5 min). After this irradiation period, the sample was rapidly warmed up to 250 K in the dark to allow mixing by convection, recooled back to 10–12 K and was further irradiated for 4 min 5–6 times. This sample thawing, recooling, and irradiation cycle was repeated once again until the sample was finally warmed to room temperature. All further manipulations of the sample were conducted using standard Schlenk line techniques. Typically, after three irradiation cycles, signals assigned either to the diazirine hemicarceplex or the diazomethane hemicarceplex could not be identified in the ^{1}H NMR spectrum of the photolyzed sample.

The photoproducts **20**–**23** were isolated and purified with semipreparative HPLC on a 250 × 10 mm LUNA silica column (Phenomenex) using 0.15% or 0.05% THF in CH_2Cl_2 at a flow rate of 5 mL min^{-1} (**20**, **21**: t_R = 15.9 min (0.15% THF); **22**, **23**: t_R = 5.3 min (0.05% THF)).

Insertion product 20: ^{1}H NMR (400 MHz, $CDCl_3$, 25 °C): δ = 6.93 (s, 2H, aryl*H*), 6.92 (s, 2H, aryl*H*), 6.85 (s, 2H, aryl*H*), 6.81 (s, 2H, aryl*H*), 5.94 (t, 1H, $OCH_{outer}(O)CH_2Ph$), 5.81 (d, 1H, $OCH_{outer}HO$), 5.75 (d, 3H, $OCH_{outer}HO$), 5.73 (d, 1H, $OCH_{outer}HO$), 5.55 (d, 2H, *o*-Ph-H), 5.42 (d, 2H, $OCH_{outer}HO$), 4.97 (t, 2H, C*H* methine), 4.90 (t, 2H, *m*-Ph-H), 4.83 (t, 1H, C*H* methine), 4.77 (t, 1H, C*H* methine), 4.64 (d, 1H, $OCH_{inner}HO$), 4.61 (t, 2H, C*H* methine), 4.48 (t, 1H, C*H* methine), 4.26 (d, 2H, $OCH_{inner}HO$), 4.23 (t, 1H, C*H* methine), 4.23 (d, 1H, $OCH_{inner}HO$), 4.1–3.8 (m, 12H, OCH_2CH_2), 3.8–3.7 (m, 4H, OCH_2CH_2, 2H, $OCH_{inner}HO$), 3.65 (t, 1H, *p*-Ph-H), 3.64 (d, 1H, $OCH_{inner}HO$), 1.6–2.38 (m, 32H, $CHCH_2CH_2$, OCH_2CH_2), 1.6–1.2 (m, 48H, $CHCH_2CH_2CH_2CH_2CH_3$), 1.20 (d, 2H, $OCH_{outer}(O)CH_2Ph$), 1.0–0.8 (m, 24H, CH_3); FAB-MS (NBA-matrix): *m*/*z* (%): 2067.7 (100) $[M+H]^+$; elemental analysis calcd (%) for $C_{127}H_{158}O_{24}$: C 73.74, H 7.70; found: C 74.04, H 7.84.

Insertion product 21: ^{1}H NMR (400 MHz, $CDCl_3$, 25 °C): δ = 6.93 (s, 2H, aryl*H*), 6.92 (s, 2H, aryl*H*), 6.85 (s, 2H, aryl*H*), 6.81 (s, 2H, aryl*H*), 5.55 (d, 2H, *o*-Ph-H), 4.97 (t, 2H, C*H* methine), 4.90 (t, 2H, *m*-Ph-H), 4.85 (t, 1H, C*H* methine), 4.77 (t, 1H, C*H* methine), 4.61 (t, 2H, C*H* methine), 4.48 (t, 1H, C*H* methine), 4.23 (t, 1H, C*H* methine), 4.1–3.8 (m, 12H, OCH_2CH_2), 3.8–3.7 (m, 4H, OCH_2CH_2), 3.65 (t, 1H, *p*-Ph-H), 2.38–1.6 (m, 32H, $CHCH_2CH_2$, OCH_2CH_2), 1.6–1.2 (m, 48H, $CHCH_2CH_2CH_2CH_2CH_3$), 1.20 (s, 1H, $OCD_{outer}(O)CH$DPh), 0.8–1.0 (m, 24H, CH_3); HR-MS: calcd for $C_{127}H_{142}O_{24}D_{16}Na$: 2106.202; found: 2106.209 $[M+Na]^+$.

Insertion product 22: ^{1}H NMR (400 MHz, $CDCl_3$, 25 °C): δ = 7.21 (t, 2H, *m*-Ph-H), 7.13 (t, 1H, *p*-Ph-H), 7.09 (d, 2H, *o*-Ph-H), 6.85–6.7 (m, 8H, aryl*H*), 5.84 (d, 1H, $OCH_{outer}HO$), 5.83–5.76 (m, 6H, $OCH_{outer}HO$), 5.74 (d, 1H, $OCH_{outer}HO$), 4.75–4.6 (m, 8H, C*H* methine), 4.49 (m, 1H, $OC(CH_2Ph)HCHH$), 4.0–3.7 (m, 15H, OCH_2CH_2), 2.95 (dd, J = 4, 13.2 Hz, 1H, CH*H*Ph), 2.67 (dd, J = 10.4, 13.2 Hz, 1H, C*H*HPh), 2.3–2.1 (m, 16H, $CHCH_2CH_2$), 2.1–1.8 (m, 15H, OCH_2CH_2), 1.73 (m, 1H, $OC(CH_2Ph)HCHH$), 1.5–1.2 (m, 48H, $CHCH_2CH_2CH_2CH_2CH_3$), 1.0–0.80 (m, 24H, CH_3); HR-MS: calcd for $C_{127}H_{158}O_{24}Na$: 2090.104; found: 2090.108 $[M+Na]^+$.

Insertion product 23: ^{1}H NMR (400 MHz, $CDCl_3$, 25 °C): δ = 7.23 (t, 2H, *m*-Ph-H), 7.13 (t, 1H, *p*-Ph-H), 7.09 (d, 2H, *o*-Ph-H), 6.85–6.7 (m, 8H, aryl*H*), 4.75–4.6 (m, 8H, C*H* methine), 4.43 (m, 1H, $OC(CH_2Ph)HCHH$), 4.0–3.7 (m, 15H, OCH_2CH_2), 2.96 (dd, J = 4.0, 13.6 Hz, 1H, CH*H*Ph), 2.66 (dd, J = 10.8, 13.2 Hz, 1H, C*H*HPh), 2.3–2.1 (m, 16H, $CHCH_2CH_2$), 2.1–1.8 (m, 15H, OCH_2CH_2), 1.73 (m, 1H, $OC(CH_2Ph)HCHH$), 1.5–1.2 (m, 48H, $CHCH_2CH_2CH_2CH_2CH_3$), 1.0–0.85 (m, 24H, CH_3); HR-MS: calcd for $C_{127}H_{132}O_{24}D_{16}Na$: 2106.202; found: 2106.207 $[M+Na]^+$.

Computations: Geometry optimizations were performed with density functional theory using the Becke3LYP[24, 25] functionals and several basis sets with the program *Gaussian 98*.[23] For the geometry and energy computations of the hydrogen-bonded complex between $^1A_1$-**3** and methanol, the geometry of $^1A_1$-**3** was constrained. Chemical shift calculations were carried out by the GIAO method, which is implemented in the program *Gaussian 98*. Chemical shifts are calculated relative to TMS which has absolute shielding values of 31.6297 (B3LYP/6-311++G(2d,2p)//B3LYP/6-31G(d)) and 32.7030 (HF/6-311+G(2d,p)//B3LYP/6-31G(d)).[46]

Acknowledgement

We warmly thank the Petroleum Research Fund administered by the American Chemical Society and Kansas State University for generous financial support. M.A.M. is very grateful to the Cancer Research Center at

  0947-6539/01/0706-1218 $ 17.50+.50/0 *Chem. Eur. J.* **2001**, *7*, No. 6

Kansas State University for an Undergraduate Cancer Research Fellowship. We thank Dr. Viatcheslav G. Zakrzewski for his help with the use of the program *Gaussian 98* and Dr. Om Prakash for assisting the NMR experiments.

[1] For reviews see: a) R. A. Moss, M. Jones, Jr., *Reactive Intermediates*, *Vol. 3*, Wiley, New York, **1985**, p. 91; b) C. Wentrup, *Reactive Molecules*, Wiley, New York, **1984**, pp. 162–264; c) P. P. Gaspar, J.-P. Hsu, S. Chari, M. Jones, Jr., *Tetrahedron* **1985**, *41*, 1479; d) R. P. Johnson, *Chem. Rev.* **1989**, *89*, 1111; e) M. S. Platz, *Acc. Chem. Res.* **1995**, *28*, 487.

[2] a) G. G. VanderStow, Ph. D. thesis, Ohio State University, Columbus (USA), **1964**; b) R. C. Joines, A. B. Turner, W. M. Jones, *J. Am. Chem. Soc.* **1969**, *91*, 7754; c) C. Wentrup, K. Wilczek, *Helv. Chim. Acta* **1970**, *53*, 1459; d) W. J. Baron, M. Jones, Jr., P. P. Gaspar, *J. Am. Chem. Soc.* **1970**, *92*, 4739; e) O. L. Chapman, J. W. Johnson, R. J. McMahon, P. R. West, *J. Am. Chem. Soc.* **1988**, *110*, 501.

[3] a) A. M. Trozzolo, R. W. Murray, E. W. Wasserman, *J. Am. Chem. Soc.* **1962**, *84*, 4991; b) P. R. West, O. L. Chapman, J.-P. LeRoux, *J. Am. Chem. Soc.* **1982**, *104*, 1779; c) R. J. McMahon, C. J. Abelt, O. L. Chapman, J. W. Johnson, C. L. Kreil, J.-P. LeRoux, A. M. Mooring, P. R. West, *J. Am. Chem. Soc.* **1987**, *109*, 2459; d) O. L. Chapman, C. J. Abelt, *J. Org. Chem.* **1987**, *52*, 1218.

[4] a) J. W. Harris, W. M. Jones, *J. Am. Chem. Soc.* **1982**, *104*, 7329; b) W. Kirmse, K. Loosen, H.-D. Sluma, *J. Am. Chem. Soc.* **1981**, *103*, 5935; c) W. Kirmse, H.-D. Sluma, *J. Org. Chem.* **1988**, *53*, 763.

[5] a) S. Matzinger, T. Bally, E. V. Patterson, R. J. McMahon, *J. Am. Chem. Soc.* **1996**, *118*, 1535; b) M. W. Wong, C. Wentrup, *J. Org. Chem.* **1996**, *61*, 7022; c) P. R. Schreiner, W. L. Karney, P. v. R. Schleyer, W. T. Borden, T. P. Hamilton, H. F. Schaefer III, *J. Org. Chem.* **1996**, *61*, 7030; d) W. L. Karney, W. T. Borden, *J. Am. Chem. Soc.* **1997**, *119*, 1378; e) D. J. Cramer, F. J. Dulles, D. E. Falvey, *J. Am. Chem. Soc.* **1994**, *116*, 9787.

[6] a) P. R. West, A. M. Mooring, R. J. McMahon, O. L. Chapman, *J. Org. Chem.* **1986**, *51*, 1316; b) S. W. Albrecht, R. J. McMahon, *J. Am. Chem. Soc.* **1993**, *115*, 855; c) P. A. Bonvallet, R. J. McMahon, *J. Am. Chem. Soc.* **1999**, *121*, 10496.

[7] a) G. B. Schuster, M. S. Platz in *Advances in Photochemistry*, *Vol. 17* (Eds.: G. Volman, G. Hammond, D. Neckers), Wiley, New York, **1992**, pp. 69–143; b) For a recent theoretical study see: W. L. Karney, W. T. Borden, *J. Am. Chem. Soc.* **1997**, *119*, 1378.

[8] B. M. Armstrong, F. Zheng, P. B. Shevlin, *J. Am. Chem. Soc.* **1998**, *120*, 6007.

[9] a) N. P. Gtitsan, T. Yuzawa, M. S. Platz, *J. Am. Chem. Soc.* **1997**, *119*, 5059; b) N. P. Gtitsan, Z. Zhu, C. M. Hadad, M. S. Platz, *J. Am. Chem. Soc.* **1999**, *121*, 1202.

[10] R. Warmuth, M. A. Marvel, *Angew. Chem.* **2000**, *112*, 1168; *Angew. Chem. Int. Ed.* **2000**, *39*, 1117.

[11] a) D. J. Cram, *Nature* **1992**, *356*, 29; b) D. J. Cram, J. M. Cram, *Container Molecules and Their Guests* (Ed.: J. F. Stoddart), Royal Society of Chemistry, Cambridge, UK, **1994**; c) E. Maverick, D. J. Cram in *Comprehensive Supramolecular Chemistry* (Ed.: F. Vögtle), Pergamon, Oxford, UK, **1996**, pp. 367–418; d) A. Jasat, J. C. Sherman, *Chem. Rev.* **1999**, *99*, 931.

[12] D. J. Cram, M. E. Tanner, R. Thomas, *Angew. Chem.* **1991**, *103*, 1048; *Angew. Chem. Int. Ed. Engl.* **1991**, *30*, 1024–7.

[13] a) R. Warmuth, *Angew. Chem.* **1997**, *109*, 1406; *Angew. Chem. Int. Ed. Engl.* **1997**, *36*, 1347; b) R. Warmuth, *Chem. Commun.* **1998**, 59.

[14] a) H. Hopf, *Angew. Chem.* **1991**, *103*, 1137; *Angew. Chem. Int. Ed. Engl.* **1991**, *30*, 1117; b) R. Warmuth, *J. Incl. Phenom.* **2000**, *37*, 1.

[15] T. Robbins, C. B. Knobler, D. Bellew, D. J. Cram *J. Am. Chem. Soc.* **1994**, *116*, 111.

[16] a) S. K. Kurdistani, R. C. Helgeson, D. J. Cram, *J. Am. Chem. Soc.* **1995**, *117*, 1659; b) J. Yoon, C. Sheu, K. N. Houk, C. B. Knobler, D. J. Cram, *J. Org. Chem.* **1996**, *61*, 9323.

[17] a) E. Schmitz, *Chem. Ber.* **1962**, *95*, 688; b) R. A. G. Smith, J. R. Knowles, *J. Chem. Soc. Perkin Trans. II* **1975**, 686.

[18] a) J. A. Bryant, M. T. Blanda, M. Vincenti, D. J. Cram, *J. Am. Chem. Soc.* **1991**, *113*, 2167; b) D. J. Cram, R. Jaeger, K. Deshayes, *J. Am. Chem. Soc.* **1993**, *115*, 10111.

[19] T. G. Savino, K. Kanakarajan, M. S. Platz, *J. Org. Chem.* **1986**, *51*, 1505.

[20] L. M. Hadel, M. S. Platz, J. C. Scaiano, *J. Am. Chem. Soc.* **1984**, *106*, 283.

[21] J. N. S. Evans, *Biomolecular NMR Spectroscopy*, Oxford University Press, New York, **1995**, pp. 71–75.

[22] The authors wish to thank Prof. Robert McMahon, Prof. Tom Bally, Prof. Peter R. Schreiner, Prof. William L. Karney, Prof. Paul v. R. Schleyer, Prof. Weston T. Borden, Prof. Henry F. Schaefer III, Prof. M. W. Wong, and Prof. Curt Wentrup for providing the geometries of **2** listed in Table 3.

[23] a) A. D. Becke, *Phys. Rev.* **1988**, *38*, 3098; b) C. Lee, W. Yang, R. G. Parr, *Phys. Rev. B* **1988**, *37*, 785; c) *Gaussian 98*, Revision A.7, Gaussian, Inc., Pittsburgh, PA, **1998**.

[24] A. D. Becke, *J. Phys. Chem.* **1993**, *98*, 5648.

[25] C. Lee, W. Yang, R. G. Parr, *Phys. Rev. B* **1988**, *37*, 785.

[26] J. Yoon, D. J. Cram, *J. Am. Chem. Soc.* **1997**, *119*, 11796.

[27] H. Günther, *NMR-Spektroskopie*, 3rd ed., Thieme, Stuttgart, **1992**, pp. 310–312.

[28] a) W. L. Karney, W. T. Borden, *Advances in Carbene Chemistry*, *Vol. 3* (Ed.: U. H. Brinker), Jai Press, London, **2000**; b) L. L. Zub, J. M. Standard, *THEOCHEM* **1996**, *368*, 133.

[29] a) T. Sugawara, H. Iwamura, H. Hayashi, A. Sekiguchi, W. Ando, M. T. H. Liu, *Chem. Lett.* **1983**, 1261; b) N. H. Werstiuk, H. L. Casal, J. C. Scaiano, *Can. J. Chem.* **1984**, *62*, 2391; c) H. L. Casal, M. Tanner, N. H. Werstiuk, J. C. Scaiano, *J. Am. Chem. Soc.* **1985**, *107*, 4616; d) R. L. Barcus, L. M. Hadel, L. J. Johnson, M. S. Platz, T. G. Savino, J. C. Scaiano, *J. Am. Chem. Soc.* **1986**, *108*, 3928; e) Y. Fujiwara, Y. Tanimoto, M. Itoh, K. Hirai, H. Tomioka, *J. Am. Chem. Soc.* **1987**, *109*, 1942; f) J. C. Scaiano, W. G. McGimpsey, H. L. Casal, *J. Org. Chem.* **1989**, *54*, 1612.

[30] D. Cremer, T. Schmidt, W. Sander, P. Bischof, *J. Org. Chem.* **1989**, *54*, 2515.

[31] a) G. Maier, W. Sauer, *Angew. Chem.* **1973**, *85*, 1056; *Angew. Chem. Int. Ed. Engl.* **1973**, *12*, 1015; b) G. Maier, *Angew. Chem.* **1974**, *86*, 491; *Angew. Chem. Int. Ed. Engl.* **1974**, *13*, 425; c) G. Maier, W. Sauer, *Angew. Chem.* **1977**, *89*, 49; *Angew. Chem. Int. Ed. Engl.* **1977**, *16*, 51.

[32] H. Irngartinger, N. Riegler, K.-D. Malsch, K.-A. Schneider, G. Maier, *Angew. Chem.* **1980**, *92*, 214; *Angew. Chem. Int. Ed. Engl.* **1980**, *19*, 211.

[33] One referee suggested the possible participation of **1** and **4** in the autoxidation of **2**.

[34] A. Krebs, H. Kimling, *Justus Liebigs Ann. Chem.* **1974**, 2074.

[35] N. J. Turro, V. Ramamurthy, K.-C. Liu, A. Krebs, R. Kemper, *J. Am. Chem. Soc.* **1976**, *98*, 6758.

[36] A. A. Gorman in *Advances in Photochemistry*, *Vol. 17* (Eds.: G. Volman, G. Hammond, D. Neckers), Wiley, New York, **1992**, pp. 215–274.

[37] We derived this rate Equation as follows. Under a steady-state approximation, the observed bimolecular rate constant k_{exptl} is $k_{exptl} = k_1k_2k_{O_2}/(k_{-1}k_{O_2}[O_2]+k_2k_{O_2}[O_2]+k_{-1}k_{-2})$ with k_1, k_{-1}, k_2, k_{-2}, and k_{O_2} as defined in Scheme 8. The rate constant k_{-2} must be much larger than $k_{O_2}[O_2]$ ($k_{-2} \gg k_{O_2}[O_2]$) otherwise the observed rate would be oxygen concentration independent. This simplifies the above equation to $k_{exptl} = k_1k_2k_{O_2}/(k_2k_{O_2}[O_2]+k_{-1}k_{-2})$. It is reasonable to assume that k_{-1} is much larger than k_2. In this case, the experimental rate constant is $k_{exptl} = K_{eq}k_{O_2}$.

[38] We exclude triplet ^{3}**1** as the reactive species for two reasons. First, the photolysis of incarcerated phenyldiazirine in an oxygenated solution does not lead to the benzene hemicarceplex in any detectable amounts. Second, the rate of the ^{3}**1** to **2** rearrangement is certainly much slower than the rate of the reaction of triplet **1** with $^3O_2$. Hence, if ^{3}**1** would react with $^3O_2$ to give **25**, the observed steady state reaction rate would be equal to the rate of the **2** to ^{3}**1** rearrangement and thus oxygen concentration independent.

[39] a) D. Cremer, J. Gauss, E. Kraka, J. F. Stanton, R. Bartlett, *J. Chem. Phys. Lett.* **1993**, *209*, 547; b) J. M. Anglada, J. M. Bofill, S. Olivella, A. Solé, *J. Am. Chem. Soc.* **1996**, *118*, 4636.

[40] P. D. Bartlett, R. Banavali, *J. Org. Chem.* **1991**, *56*, 6043.

[41] Preliminary experiments show that incarcerated 5-methylcycloheptatetraene, which is equally strained as **2**, reacts 7.4 times faster with triplet oxygen as compared to incarcerated **2**; this suggests the possibility of an initializing electron transfer step in this reaction (J.-L. Kerdelhué, R. Warmuth, unpublished results).

[42] a) J. E. Leffler, *J. Org. Chem.* **1955**, *20*, 1202; b) J. E. Leffler, E. Grunwald, *Rates and Equilibria of Organic Reactions*, Wiley, New York, **1963**; reprinted: J. E. Leffler, E. Grunwald, *Rates and Equilibria of Organic Reactions*, Dover, New York, **1989**; c) R. Schmid, V. N. Sapunov in *Non-Formal Kinetics*, *Monographs in Modern Chemistry* (Ed.: H. F. Ebel), VCH, Weinheim, **1982**.

[43] a) E. Grunwald, *Thermodynamics of Molecular Species*, Wiley, New York, **1996**; b) E. Grunwald, C. Steel, *J. Am. Chem. Soc.* **1995**, *117*, 5687; c) C. Reichardt, *Solvents and Solvent Effects in Organic Chemistry*, 2nd ed., VCH, Weinheim, **1988**.

[44] a) R. G. Chapman, J. C. Sherman, *J. Am. Chem. Soc.* **1999**, *121*, 1962; b) R. G. Chapman, J. C. Sherman, *J. Org. Chem.* **2000**, *65*, 513.

[45] a) R. Lumry, S. Rajender, *Biopolymers* **1970**, 1125; b) R. Lumry, R. B. Gregory in *The Fluctuating Enzyme* (Ed.: G. R. Welch), Wiley, New York, **1986**.

[46] J. B. Foresman, A. Frisch, *Exploring Chemistry with Electronic Structure Methods*, 2nd ed., Gaussian Inc., Pittsburgh, PA, **1996**.

Received: August 7, 2000 [F2652]

0947-6539/01/0706-1220 $ 17.50+.50/0